ELSEVIER

Magnetic Resonance Imaging, Vol. 15, No. 8, pp. 917–927, 1997

Printed in the USA.
0730-725X/97 $17.00 + .00

PII S0730-725X(97)00002-7

● *Original Communication*

AUTOMATIC ANALYSIS OF CEREBRAL ATROPHY

GERARD SUBSOL,* NEIL ROBERTS,† MARK DORAN,‡ JEAN-PHILIPPE THIRION,* AND GRAHAM H. WHITEHOUSE†

*Institut National de Recherche en Informatique et en Automatique (INRIA), Project Epidaure, Sophia Antipolis, France, †Magnetic Resonance and Image Analysis Research Centre, University of Liverpool, UK, and ‡Walton Centre for Neurology and Neuroscience, Walton Hospital, Liverpool, UK

3D MR data obtained for 10 healthy control subjects have been used to build a brain atlas. The atlas is built in four stages. First, a set of features that are unambiguously definable and anatomically relevant need to be computed for each item in the database. The chosen features are crest lines along which the maximal principal curvature of the surface of the brain is maximal in its associated principal direction. Second, a nonrigid registration algorithm is used to determine the common crest lines among the subjects in the database. These crest lines form the structure of the atlas. Third, a set of crest lines is taken as a reference set and a modal analysis is performed to determine the fundamental deformations that are necessary to bring the individual data in line with the reference set. The deformations are averaged and the set of mean crest lines becomes the atlas. Finally, the standard deviation of the deformations between the atlas and the items in the database defines the normal variation in the relative positions of the crest lines in a healthy population. In a fully automatic procedure, the crest lines on the surface of the brain adjacent to the cerebral ventricles in a patient with primary progressive aphasia were compared to the atlas; confirmation that the brain of this patient demonstrates atrophy was provided by stereological analysis that showed that the volume of the left cerebral hemisphere is 48.8 ml (CE 2.8%) less than the volume of the right cerebral hemisphere in the region of the temporal and frontal lobes. When the amplitude of the deformations necessary to register the crest lines obtained for the patient with the atlas were greater than three standard deviations beyond the variability inherent in the atlas, the deformation was considered significant. Four of the five main deformation modes of the longest crest line of the surface of the brain adjacent to the cerebral ventricles were significantly different in the patient with primary progressive aphasia compared to the atlas. The ventricles are preferentially enlarged in the left cerebral hemisphere. Furthermore, they are closer together posteriorly and further apart anteriorly than in the atlas. These observations may be indicative of the atrophy of the temporal and frontal lobes of the left cerebral hemisphere noted in the patient. Ultimately, the approach may provide a useful screening technique for identifying brain diseases involving cerebral atrophy. Serial studies of individual patients may provide insights into the processes controlling or affected by particular diseases. © 1997 Elsevier Science Inc.

Keywords: **Atlas; Atrophy; Brain; Cerebral ventricles; Crest lines; Image analysis; MRI; Stereology.**

INTRODUCTION

The main purpose of medical imaging is to assist in the diagnosis of disease. Serial investigations allow the efficacy of treatments to be monitored and may be more frequently performed by Magnetic Resonance (MR) imaging because this technique does not employ ionizing radiation. MR images are inherently digital and, therefore, amenable to computer-based image analysis techniques. Accordingly, the term "evidence-based medicine" has been coined reflecting the fact that decisions regarding diagnosis and assessment of treatment response can be based on increasingly objective criteria. There is also the possibility that measure-

RECEIVED 7/23/96; ACCEPTED 2/7/97.
Address correspondence to Dr. Neil Roberts, Magnetic Resonance and Image Analysis Research Centre, University of Liverpool, P.O. Box 147, Liverpool, L69 3BX, UK

ments on MR images can be made automatically. Here we describe how image analysis algorithms applied to 3D MR data obtained for the brain in a group of healthy subjects have been used to construct an atlas describing the mean size, shape, and inherent biological variation in the brain in a normal population. Subsequently, 3D MR data obtained for a patient with a focal cortical syndrome known as Primary Progressive Aphasia (PPA) have been automatically analyzed in respect of the atlas.

In focal cortical syndromes a circumscribed cognitive deficit such as gradual loss of speech develops insidiously over many years and progresses without evidence of involvement of other cognitive domains. These syndromes have a considerable theoretical interest, as they allow detailed study of the breakdown of specific cognitive functions in isolation. Furthermore, because of a clear asymmetric pattern of tissue loss, focal syndromes represent useful paradigms from which to develop a method for measurement of atrophic processes. Qualitative inspection of single MR images[1] or computed surface renderings may reveal significant atrophy, but both methods may be insensitive to small changes, and the renderings are particularly problematic in that widening deep within the sulci may not be revealed. Application of the Cavalieri method of modern design stereology with associated point counting techniques[2,3] represents a convenient and unbiased method for rapidly quantifying the extent of cerebral atrophy. It may be applied to measure differences in the volume of the whole brain relative to a normative database or to compare the volumes of the left and right cerebral hemispheres. When the volume differences are greater than 5% their detection requires only moderate workloads of 5–10 min point counting on 5–10 systematic sections. The present study investigates whether automatic analysis of the shape of the brain may also provide a useful means of detecting and studying cerebral atrophy. First, computer-based image analysis techniques have been used to segment the brain in 3D MR data obtained for 10 healthy control subjects. Subsequently, crest lines (sometimes called ridge lines) have been computed joining points where the maximal principal curvature of the surface of the brain is maximal in its associated principal direction, and averaged to provide an atlas against which deformations of the brain occurring in patients with cerebral atrophy may be recognized and studied. In particular, deformations of the shape of the brain adjacent to the lateral cerebral ventricles in a patient with PPA are analyzed.

Enlargement of the cerebral ventricles is well established as an indicator of cerebral atrophy. One of the earliest reports of its measurement in vivo was by Evans,[4] who determined the ratio of the distance between the horns of the left and right lateral ventricles divided by the maximum internal skull width. This ratio was obtained from CT images in investigations of the variability in the size of the ventricles in large populations of adults and children.[5,6] Linear measurements[7,8] and planimetric measurements,[9] on CT images have also been used to assess age-related changes in the cerebral ventricles. More recent studies have employed the Cavalieri method in combination with point counting to estimate the volume of the cerebral ventricles on CT[10] and MR images.[11] The latter study reports good agreement between the results of manual point counting and automated image analysis techniques in estimating ventricular volume. A study of age-related changes in the volume of the cerebral ventricles, using image analysis techniques applied to MR images, has shown that linear increases in the volume of the ventricles are accompanied by a substantial reduction in cortical gray matter with advancing age.[12]

The above-mentioned age-related changes and the inherent variability in the size and shape of the brain in a normal population mean that caution needs to be exercised in setting too low a threshold with respect to which differences in the brain of the patient with PPA relative to the atlas might be considered significant. The atlas does, however, represent a useful reference in respect of which to begin to automatically screen for the presence of cerebral atrophy. Moreover, the actual deformation modes exhibited by the crest lines on the boundary between the brain and the lateral cerebral ventricles may be sufficiently sensitive to differentiate between different atrophic processes. For example, they can indicate whether atrophy has preferentially affected the left or right hemisphere, and possibly, more specifically, indicate whether, for example, the temporal or frontal lobe is involved.

MATERIALS AND METHODS

Subjects

The patient is a 65-yr-old man referred by his GP with a progressive loss of language (i.e., aphasia). Previous investigations, which included a CT scan, EEG, and psychiatric assessment, failed to identify a structural or psychiatric cause for his aphasia. The results of a routine dementia screening examination were all normal or negative. In all cognitive domains other than language he performed normally and was able to successfully manage the activities of daily living. His episodic memory and behavior were normal.

Detailed neurological and psychometric assessment

of the patient resulted in the diagnosis of Primary Progressive Aphasia (PPA). Patients with the fluent variety of PPA (also described as semantic aphasia) produce flowing sentences, but because of anomic difficulties these sentences do not make sense. However, the patient for whom MR data were obtained in the present study possesses nonfluent PPA, so that although he has difficulty in putting grammatically correct sentences together, there is no evidence of comprehension or confrontation naming impairments. Furthermore, progressive dysfluency has resulted in a severely restricted verbal output, such that utterance length is now rarely greater than a single word. The patient also possesses a second deficit, namely phonological dyslexia, whereby he is unable to read nonwords.

Magnetic Resonance Imaging

MR images of the patient were obtained at the Magnetic Resonance and Image Analysis Research Centre in the University of Liverpool, using a T_1-weighted radio frequency spoiled gradient echo (SPGR) sequence available on a 1.5 T SIGNA whole-body MR imaging system (General Electric, Milwaukee, WI). One hundred and twenty-four coronal images referring to 1.6 mm thick contiguous sections have been obtained through the brain using a proprietary birdcage head coil. The protocol employed a repetition time (TR) of 34 ms, echo time (TE) of 9 ms and flip angle of 45°. The Field of View (FOV) of each image was 20 cm. The images were acquired with a matrix comprising 256 readings of 128 phase encodings with 1 excitation per phase encoding (NEX), in 14 min 26 s. A systematic series of coronal sections reformatted (see below) from the 3D data are shown in Fig. 1. For routine diagnostic purposes, a series of T_2-weighted images was also obtained to allow detection of the presence of any focal pathological changes. The appearance of these images is normal.

The brain atlas was constructed from 3D MR data sets obtained for 10 healthy male subjects of mean age 37 years at the Brigham and Women's Hospital, Boston, MA, using the same imaging protocol as that used for the patient. All 10 subjects were right-handed and none had a history of psychiatric or neurological illness or alcohol abuse. The subjects served as age-matched controls for a group of schizophrenic patients studied by Shenton and colleagues.[13]

Stereological Analysis of Cerebral Atrophy

The MR images obtained for the patient were transferred to ANALYZE software (MAYO Foundation, MN)[14] running on a SPARC 10 workstation (SUN Microsystems, CA). The 256 × 256 × 124 acquired voxels were linearly interpolated to an array of 256 × 256 × 254 isometric (i.e., cubic) voxels of side 0.78 mm. These data were then reformatted to produce a series of image planes all lying along a direction parallel to the long axis of the hippocampus, which represents a convenient orientation for comparison of measurements obtained from different subjects.[15]

Estimates of the section area (A) of the transects through the left and right cerebral hemispheres on selected images were obtained using manual point counting techniques (see, e.g., Roberts et al.[3]). These techniques are available in a purposely designed interface (Fig. 2) within the ANALYZE software (MAYO Foundation, MN). Provided that the test system is placed at random on the image, an unbiased estimate of the transect area is obtained as the sum of the points overlying the cerebral hemisphere multiplied by the area associated with each point (i.e., the area of the grid squares that would be formed if the line segments in Fig. 2 were joined). Point counting was performed by a clinician (MD) experienced in assessing the appearance of the brain on MR images. Measurements were made on every fifth image between slices 50 and 210, thus focusing the study in a broad central region of the brain. For estimation of the volume of the whole cerebral hemisphere, one throw of the test system used for point counting on each of approximately 10 systematic sections that exhaustively sample the brain would be sufficient to produce a Coefficient of Error (CE) on the volume estimate of better than 5%. However, on this occasion it is of interest to compare the section areas of the left and right cerebral hemispheres on each image. Accordingly, the preferred sampling strategy has been to repeat the point counting procedure eight times on each section using a rather sparse grid such that about 15 points are counted per grid throw. The average value from the eight throws, based on a total of slightly more than 100 point counts, is a suitably precise estimate of the required section area. Additionally, the boundary length (B) of the transects was estimated by intersection counting so that values of the dimensionless shape coefficient $B/\sqrt{A}$ (see, Pache and colleagues[16]) could be computed for each hemisphere on each section.

Automatic Analysis of the Size and Shape of the Cerebral Ventricles

Building the brain atlas. The raw data used in the construction of the brain atlas were obtained by application of mathematical morphology algorithms to segment the brain in the 3D MR data sets obtained for 10 healthy control subjects. The atlas takes into account

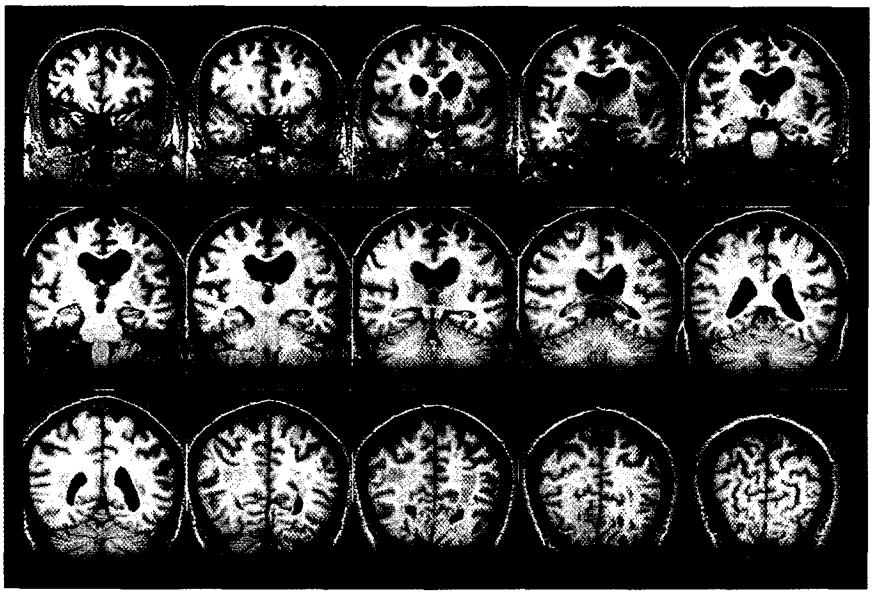

Fig. 1. Series of systematic coronal sections, approximately every 8 mm, through the central portion of the brain of a patient diagnosed as possessing nonfluent PPA and phonological dyslexia. Visual inspection of the images demonstrates a reduction in brain tissue in the left cerebral hemisphere (right side of each panel) and is especially noticeable in the two rightmost panels of the upper row and the two left-most panels of the middle row. The cerebral ventricle also appears enlarged in the left hemisphere, and this is especially noticeable in the two right-most panels of the upper row and the two left-most panels of the bottom row.

Fig. 2. A stereological test system for point counting is shown overlain on the MR image corresponding to the top-right panel of Fig. 1. A magnified portion of the image in the region of the left lateral ventricle is shown in the right bottom. Those points that overlie cerebral tissue are recorded for each hemisphere separately. The procedure was repeated five times for sections separated by approximately 4 mm in the central portion of the brain.

the resemblances as well as the diversity of the items of the database. It can be defined as a set of landmark features that are common (i.e., present in all the individual data) and invariant (i.e., in the same relative position in each individual). There are five main steps in its construction:

1. Feature extraction: the features that will constitute the atlas need to be extracted from the segmented 3D MR data. Ideally, the relevant features will be unambiguously definable and anatomically relevant. The chosen features are crest lines that are mathematically defined as joining points of zero maximal principal curvature and may be computed by the Marching Lines Algorithm.[17,18] On the cortical surface they match the anatomically defined pattern of gyri and sulci. The mathematical definition of crest lines is based on a continuous (i.e., nonvoxelated) description of a surface and, therefore, it is necessary to convolve the discrete values of the image with a Gaussian function to obtain a continuous representation. A tradeoff between smoothing and localization is necessary in setting the value of the Gaussain parameter, σ. A simplified multiscale scheme is used. Sets of crest lines are extracted with low and high values of σ (i.e., 1.5 and 4.5). The two sets are registered, and those crest lines that coincide form a set of crest lines that are appropriately positioned and smooth.
2. Feature registration: the sets of crest lines computed for the different subjects in the database need to be registered with each other in turn. This involves a nonrigid registration algorithm based on the Itera-

tive Closest Point Method,[19,20] extended to include a sequence of 5 rigid, 5 affine, and 10 spline deformations, and applied to the first data set to superimpose it on the second. The point-to-point correspondences between the two data sets are thus obtained. Crest lines referring to gyri and sulci may be readily separated because they correspond to maximal curvatures that are respectively positive and negative.

3. Common feature identification: once the common crest lines have been nonrigidly registered, their correspondences between pairs of subjects in the database is assessed. Two crest lines are considered a common feature between the two data sets when a given proportion (35% in our application) of the points of one of the crest lines is matched with the points of the other. The pairwise registrations produce a subset of crest lines that is common to all the subjects. These common crest lines form the basis of the atlas. It is possible to manually label each feature in one of the data sets with a code reflecting, for example, its anatomical name. This labeling is then automatically propagated to all the data sets, so that it is then possible to extract the points on the surface of the brain that are close to the lines with a given label. Accordingly, different anatomical regions can be highlighted (see, e.g., the rendering of the cerebral ventricles in later Fig. 5).
4. Feature average position: the mean position of crest lines constituting the atlas is determined by averaging the sets of 3D crest lines defining each common subset. This produces a 'smooth' set of crest lines, each composed of typically 50 to 200 points. Next, a set of crest lines is taken as a reference set ($\mathcal{R}$) and the isotropic scaling transformations and rigid (i.e., translations and rotations) and nonrigid deformations between the crest lines ($\mathcal{L}$) of the reference set and the corresponding lines of the other data sets are computed. For each line $\mathcal{L}$ of $\mathcal{R}$ the point-to-point correspondences with the common lines of the other data sets are determined. This analysis gives the deformations between $\mathcal{L}$ and the other data sets. The deformations are analyzed by modal analysis[21–23] and decomposed into fundamental deformation modes that are made up of cosine terms of decreasing spatial frequency. The amplitudes of the modes are averaged to determine the 'mean' deformation and this is applied to $\mathcal{L}$ to produce the 'mean' crest line of the atlas. By using point correspondences between $\mathcal{R}$ and the atlas, a volumetric spline transformation[24] may be defined that can be applied to $\mathcal{R}$ in order to produce a surface representation of a hypothetical brain corresponding to the atlas.
5. Feature variability analysis: it is assumed that all the items in the database are 'normal' and, having found the average position of the crest lines constituting the atlas, the remaining step is to define the range of normal deformations inherent in the database. The crest lines of the atlas are registered with each of the individual data sets in turn, and the modal decomposition of all these deformations is computed for orthogonal coronal, sagittal, and axial projections. Then, in each projection the average amplitude Δ_A and its associated standard deviation σ is calculated for each line and for each mode.

Using the brain atlas. The comparison between the patient data and the atlas is in three steps. Crest lines are computed for the brain of the patient. Next, a nonrigid registration is used to find the common crest lines between the atlas and the patient data. It then becomes possible to superimpose the patient data on the atlas so that pathology may be visualized in respect of the normality defined by the atlas. Because some of the crest lines of the atlas have been manually labeled, it is possible to propagate the labels to the patient crest lines in order that specific parts of the brain may be automatically identified and studied. In particular, the longest crest line of the left and right cerebral ventricles represents a common anatomically relevant feature in both the atlas and the patient data that is convenient for analysis in respect of the present detail of the atlas. The amplitudes of the first five deformation modes of this crest line in the patient relative to the atlas were calculated and compared with the 'normal' modal amplitude. By using a χ^2 test, differences that are not in the average range, and thus represent 'abnormal' deformations, could be identified and analyzed. Thus the 'abnormal' deformations are detected automatically via a mathematical analysis in which the several hundred point deformation vectors defining anatomical differences are replaced by a handful of parameters. In spite of their mathematical definition, some of the deformations can be visualized intuitively as is described below.

The CPU-time for extracting crest lines from a volumetric image is approximately 30 min on a DEC-Alpha workstation. The registration of the two sets of crest lines, of which there are typically 2,000 per data set, each comprising 30,000 points, takes about 20 min. Application of the algorithms to construct the atlas needs to be performed only once and takes several hours. The study of individual patients relative to the atlas comprises, automatic labeling, superimposition, and deformation analysis, and takes about 1 h.

RESULTS

The results of the stereological analysis that are presented in Fig. 3a–c reveal a highly significant hemispheric asymmetry in the patient with PPA such that over 8 cm of coronal sections the volume of the left cerebral hemisphere is significantly reduced relative to the right. Figure 3a shows the individual values of the section areas of the left and right hemisphere obtained from the eight throws of the point counting test system on each image, and in Fig. 3b the mean of these values and the associated standard error are plotted. The atrophy of the left frontal and temporal lobes in the patient has produced a difference of 48.8 mls (CE 2.8%) between the volume of the left and right cerebral hemispheres. The data of Fig. 3c indicate that the value of the dimensionless shape coefficient $B/\sqrt{A}$ is preferentially increased in the portion of the brain where the left cerebral hemisphere has reduced volume, indicating that here cerebral atrophy has caused the sulci to be deeper and the gyri narrower than usual.

The crest lines of the patient shown in Fig. 4b and d were automatically registered with the atlas constructed from MR data obtained for 10 healthy control subjects shown in Fig. 4e and f. The superimposition of the ventricles of the atlas and the patient in the upper two panels of Fig. 5 clearly shows that the patient ventricles are bigger and asymmetric. The analysis of the significance of the first five deformation modes of the longest crest line of the surface of the brain adjacent to the left and right cerebral ventricles in the axial plane is presented in Table 1. Those deformations that are further than 3 standard deviations from the average value are considered significant. A summary of the significant deformations of the longest crest line of the surface of the brain adjacent to the left and right cerebral ventricles in the axial, sagittal, and coronal planes is presented in Table 2. In the lower left and right panels of Fig. 5 the significant deformations are applied separately to the crest line in the axial and sagittal plane, respectively, and the deformation they create compared to the atlas. In the axial plane (bottom left panel), it is Mode 1 that is significant for both the left and right hemispheres. Whereas Mode 0 corresponds to a displacement of the whole crest line, Mode 1 corresponds to a single cosine term applied along the length of the axial projection of the crest line, so that, in broad terms, half of the length of the crest line is displaced in one direction while the other half is displaced in the opposite direction. Thus, we observe that, compared to the atlas, the left and right ventricles are closer together posteriorly and further apart anteriorly, as indicated by the black arrows in Fig. 5. This observation may be indicative of the abovementioned finding of preferential atrophy of the anterior portion of the left cerebral hemisphere in this patient. In the sagittal plane, Modes 0, 1, and 4 are significant for the longest crest line on the surface of the brain adjacent to the left ventricle, while only Modes 1 and 4 are significant for the longest crest line adjacent to the right ventricle. Mode 0 constitutes an upwards displacement, and Mode 1 and Mode 4, respectively, comprise one and four cosines terms of decreasing period applied along the length of the sagittal projection of the crest line. The overall effect of these terms, which corresponds to a significant enlargement of the left cerebral ventricle, is displayed in the bottom right panel of Fig. 5.

The stereological and image analysis techniques represent two robust and complementary techniques for making useful analyses of 3D MR data. The stereological approach allows simple, fast, manual, unbiased estimation of the volume of the left and right cerebral hemispheres with known precision. The more sophisticated image analysis techniques provide insights into the displacements and deformations of the brain that occur as a result of cerebral atrophy.

DISCUSSION

In 1836 clinical observations led Marc Dax to express the idea of the dominance of the left hemisphere for language and in 1860, based on the results of pathological analysis, Paul Broca[25] reported that aphasia resulted from a lesion to the left inferior frontal gyrus. The concept of cerebral dominance was subsequently substantiated by frequent observations that unilateral brain damage produces material specific psychological deficits (see review by Hellige[26]) and it is now accepted that the left and right cerebral hemispheres are respectively more important for handling verbal and nonverbal information. It was, therefore, expected that the patient would show evidence of left hemisphere atrophy reflecting his language difficulties, and this is confirmed. The reduction in volume of the left hemisphere demonstrated by the sterological analysis has two underlying components, which are of increasing relative importance between sections 80 and 180 in Fig. 3, i.e., left frontal lobe atrophy, which most probably corresponds to the patient's nonfluent PPA[27] and left temporoparietal lobe atrophy, which most probably corresponds to his phonological dyslexia.[28] On this occasion it would, therefore, have been possible to automatically screen for the presence of significant cerebral atrophy in the patient that is consistent with his being diagnosed with PPA.

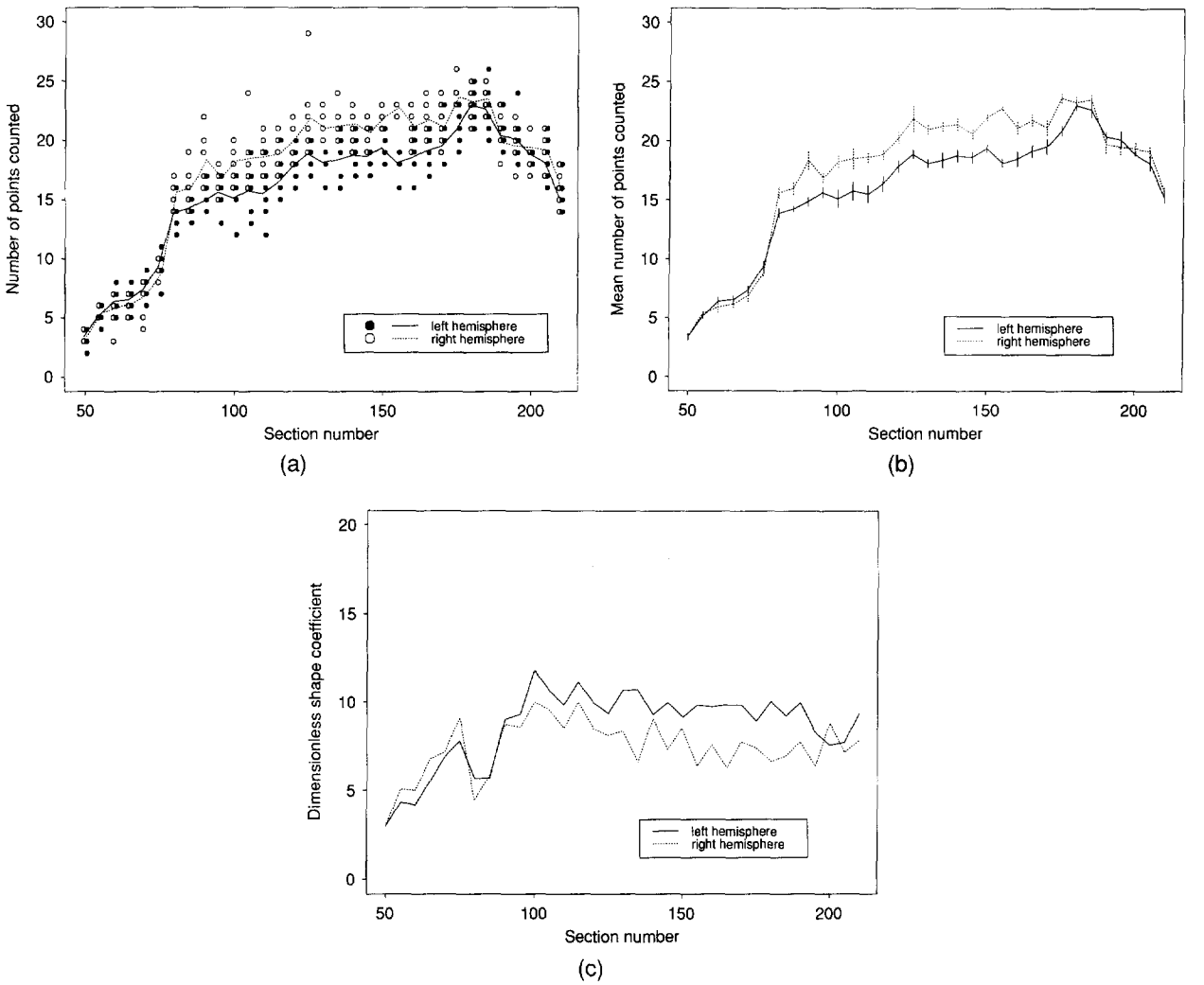

Fig. 3. (a) Individual values of the section area obtained from eight throws of the point counting test system are plotted against section number in the central portion of the brain of the patient with PPA. (b) The mean value of the section area obtained from eight repeat throws of the test system is plotted against section number. The error bar on each point corresponds to 1 standard error on the estimate. The section area in the left cerebral hemisphere is significantly reduced in comparison to the right cerebral hemisphere over a region of approximately 8 cm. (c) Plot of the value of the dimensionless shape coefficient $B/\sqrt{A}$ for the same sections as in (a) and (b). The value of $B/\sqrt{A}$ is preferentially increased in the portion of the brain where the left cerebral hemisphere has reduced volume. Cerebral atrophy has caused the sulci to be deeper and the gyri narrower than usual.

The analysis could eventually be extended to include all of the crest lines shown in the top two panels of Fig. 4, but this requires that a more detailed atlas is constructed. The deformation modes obtained for individual cerebral gyri could then be used to automatically determine the regions of the cerebral hemisphere specifically affected in PPA. However, differences in the arrangement of the gyral and sulcal pattern of the brain between individuals mean that the interpretation of the deformation modes of crest lines of individual gyri is not straightforward. Whereas stereological analysis of regional brain volumes is a proven method finding increasing neuroimaging applications, the analysis of crest lines is a new approach and the present study is the first description of its use for a real clinical application. The promising results obtained should encourage the development of the approach. For example, more sophisticated methods for determining the significance of the deformations need to be developed. Furthermore, it has been assumed that the deformation modes are uncorrelated. Assessment of the significance of the deformations by Principal Component Analysis may be a way to make progress away from this assumption. Developments in MR imaging protocols to produce higher resolution data sets would also make the

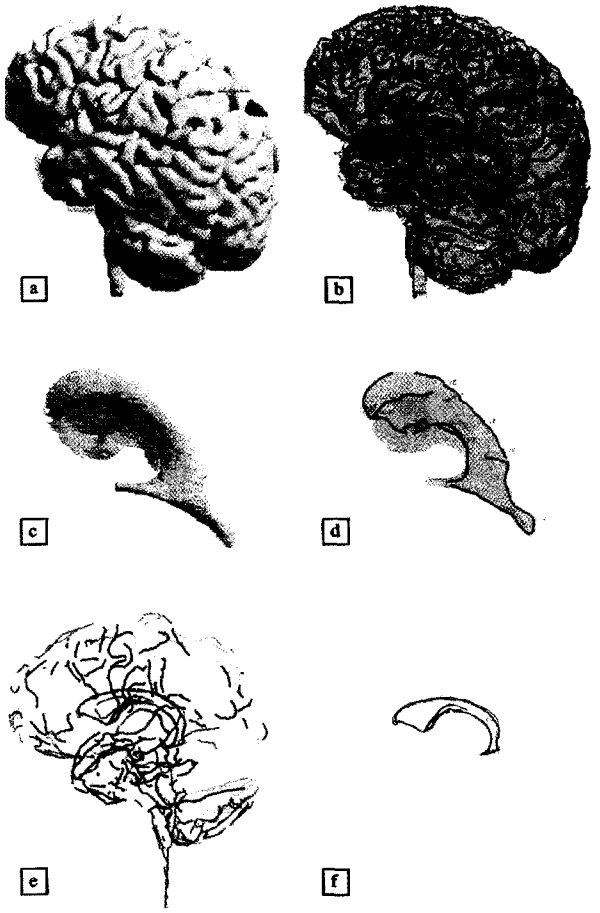

Fig. 4. Models of the brain (a) and cerebral ventricles (c) of the focal aphasic patient produced by volume rendering techniques applied to 3D MR data. In (b) and (d) crest lines computed for the surface of the brain are shown overlain in blue on the volume renderings of these structures. The corresponding crest lines of a brain atlas constructed from a database of ten healthy control subjects, are shown in red in (e) and (f), respectively. It should be noted that the lateral horns of the cerebral ventricles are frequently so small as to comprise only a few image pixels and are thus not represented in the segmented image.

analysis of crest lines obtained for individual gyri more feasible.

The extent to which the techniques reported in this article might be further developed and routinely used for automated diagnosis depends on whether the MR investigations of relevant patients employ volumetric or multislice protocols. In multislice acquisitions, series of 10 to 20 images, which typically refer to tissue sections of 5 to 10 mm thickness are acquired, occasionally contiguously, but more usually with a gap of 5 to 20 mm between sections and with an in-plane resolution (i.e., pixel width) of between 0.75 and 1 mm. In a volumetric, or 3D, acquisition, the images possess similar in-plane resolution to the multislice images but now the tissue sections are always contiguous and only 1 to 2 mm thick. Typically, 3D acquisitions yield series of 124 images and encompass the whole brain. Radiologists, will generally specify the use of multislice protocols for two reasons. They provide images with good signal-to-noise ratio and optimum contrast between different tissue types in imaging times of about 5 min. Volumetric data are, however, a prerequisite if automatic analysis of the shape of the brain is to be performed. Until recently, volumetric acquisitions have generally produced images with inferior signal-to-noise ratio, and contrast-to-noise ratio, in a minimum time of about 15 min, so as to have generally only been used in special examinations such as Magnetic Resonance Angiography (MRA) where the relevant contrast between tissue and blood vessels is inherently high. The situation is changing, acquisition times for 3D data have been reduced to between 5 and 10 min and considerably more flexibility is available for developing optimum contrast between different tissue types. For example, the 3D Fast IR-Prepped GRASS sequence provides greater T_1-weighting than

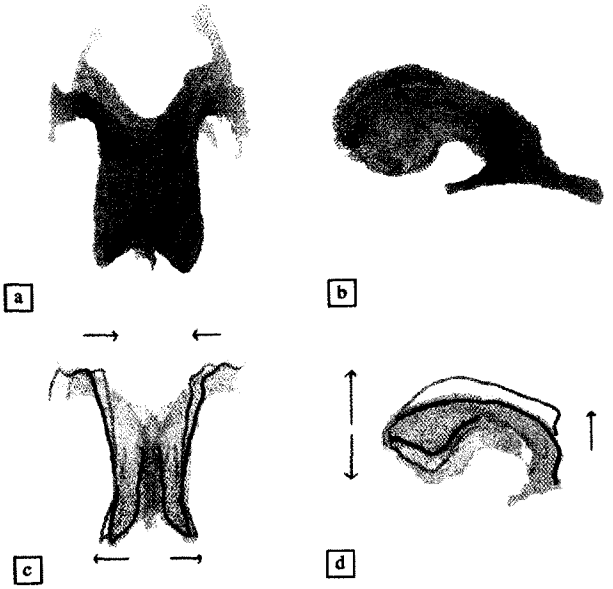

Fig. 5. A computer rendering of the cerebral ventricles of the PPA patient are shown in blue overlain on the atlas in red, in transverse (a), and coronal (b) views. In (c) and (d) the positions of the principal crest line of the surface of the brain adjacent to the left and right cerebral ventricles in the patient and atlas are shown in blue and red, respectively. The short black arrows indicate the directions of the deformations of the patient data relative to the atlas.

Table 1. The amplitudes of the displacements, Δ, of the first five deformation modes of the longest left and right ventricular crest line of the atlas toward the patient

	Mode 0	Mode 1	Mode 2	Mode 3	Mode 4
Left					
Δ	−9.11	−60.90	32.82	−35.44	−4.71
Δ_A	−0.06	2.28	0.21	−4.76	1.81
σ	20.27	12.32	17.09	14.33	3.42
$(\Delta - \Delta_A)/\sigma$	−0.446	**−5.128**	1.908	−2.141	−1.906
Right					
Δ	−21.22	72.67	−39.98	22.53	12.69
Δ_A	−4.67	6.43	−5.35	4.56	−4.45
σ	26.23	15.16	25.36	11.21	3.63
$(\Delta - \Delta_A)/\sigma$	−0.631	**4.369**	−1.787	1.603	**4.722**

The deformation mode is considered significant when its amplitude is outside 3 standard deviations σ from the mean value, Δ_A, obtained by deforming the atlas toward each of the individuals from which it is constructed ($p = 0.01$). Those deformation modes considered to be significant are indicated in bold. The data in this table all correspond to deformations in the axial plane.

the 3D SPGR sequence used in the present study. In addition, the 3D Fast Spin Echo (FSE) sequence can provide T_2-weighting. It is likely that in future 3D data sets will be acquired in clinical practice more frequently than they are today. Of course, it is also possible that the prospect of automated analyses may influence the sorts of MR data that are acquired. In particular, the 3D FSE protocol, as well as producing MR images in which tissue pathologies are generally well visualized, provides excellent contrast between high signal intensity CSF and lower signal intensity brain tissue. This contrast plays in favor of obtaining a reliable segmentation and subsequent analysis of the morphology of the brain.

Table 2. The results of the analysis of the significance of the first five deformation modes of the longest crest line of the left (LV) and right (RV) cerebral ventricles in the patient with PPA relative to the brain atlas

	Mode 0	Mode 1	Mode 2	Mode 3	Mode 4
LV_A	−0.446	**−5.128**	−1.908	−2.141	−1.906
RV_A	−0.631	**4.369**	−1.787	1.603	**4.722**
LV_S	**3.687**	**8.667**	0.451	0.736	**−5.081**
RV_S	−1.242	**8.336**	−0.999	0.757	**−5.233**
LV_C	**4.429**	−1.297	**−3.731**	−0.186	−1.442
RV_C	0.309	1.824	**−5.590**	1.986	−0.581

Deformations in the axial, sagittal, and coronal planes are indicated by the subscripts A, S, and C, respectively. Those deformation modes considered to be significant are indicated in bold. The deformations corresponding to LV_A and RV_A, and LV_S are illustrated in the left and right bottom panels of Fig. 5, respectively. The data presented in the top two rows of this table are identical to the bottom rows of the upper and lower portions of Table 1, respectively.

While the thrust of the present article has been to illustrate the clinical utility of atlases constructed from 3D MR data, an alternative interesting application is to study and quantify the developmental changes that occur in the convolution patterns of gyri and sulci in the brain during childhood through to old age, and to consider whether the patterns are inherently different in males than females,[29] or in groups with a predisposition to particular diseases such as schizophrenia.[30]

The possibility of using 3D images to generate atlases providing baselines against which to pursue the possibility of automatic diagnoses is not restricted to the brain. Previous applications of the techniques described in this article include the development of a skull atlas from 3D CT data obtained for specimen skulls.[31] This atlas was used to study the deformation that had occurred in the skull of a patient with Crouzon's disease. The skull atlas may also provide a useful baseline in respect of which to study the evolutionary changes depicted in fossil hominid skulls.

Further work is in progress to obtain 3D MR data sets for a larger group of normal subjects, so that eventually separate atlases will be constructed for male and female subjects and also for different age ranges. The possibility of using robust features other than crest lines for constructing the atlases is also being explored. A promising alternative is to use the lines produced from a 3D skeletonization of the segmented objects.[32] In addition, alternative methods of shape analysis are being explored. These include the Finite Element Method,[23] Principal Warps,[33] Fourier Analysis,[32] and Principal Component Analysis.[34] The application of stereological methods to determine geometric parame-

ters such as the surface area of the brain and the spatial distribution of this and other geometric quantities is also being addressed.

Acknowledgments—The 3D MR data used to construct the brain atlas used in this study were provided by Dr. Martha Shenton and Dr. Robert W. McCarley of the Department of Psychiatry, Harvard Medical School, Boston, MA.

REFERENCES

1. Caselli, R.J.; Jack, C.R.; Petersen, R.C.; Walker, H.W.; Yanpagihura, T. Asymmetric cortical degenerative syndromes. Neurology 42:1462–1468; 1992.
2. Gundersen, H.J.G.; Jensen, E.B. The efficiency of systematic sampling in stereology and its prediction. J. Microsc. 147:229–263; 1987.
3. Roberts, N.; Garden, A.S.; Cruz-Orive, L.M.; Whitehouse, G.H.; Edwards, R.H.T. Estimation of fetal volume by magnetic resonance imaging and stereology. B. J. Radiat. 67:1067–1077; 1994.
4. Evans, W.A. An encephalographic ratio for estimating ventricular enlargement and cerebral atrophy. Arch. Neurol. 47:931–937; 1942.
5. Glydensted, C. Measurements of the normal ventricular system and hemispheric sulci of 100 adults with computed tomography. Neuroradiology 14:183–192; 1977.
6. Pedersen, H.; Glydensted, M.; Glydensted, C. Measurements of the normal ventricular system and supratentorial subarachnoid space in children with computed tomography. Neuroradiology 17:231–237; 1979.
7. Hahn, F.J.Y.; Rim, K. Frontal ventricular dimensions on normal computed tomography. AJR 126:593–596; 1976.
8. Haug, G. Age and sex dependence of the size of normal ventricles on computed tomography. Neuroradiology 14:201–204; 1977.
9. Barron, S.A.; Jacobs, L.; Kinkel, W.R. Changes in size of normal ventricles during aging determined by computerized tomography. Neurology 26:1011–1013; 1976.
10. Pakkenberg, B.; Boesen, J.; Albeck, M.; Gjerris, F. Unbiased and efficient estimation of total ventricular volume of the brain obtained from CT-scans by a stereological method. Neuroradiology 31:413–417; 1989.
11. Keshaven, M.S.; Anderson, S.; Beckwith, C.; Nash, K.; Pettegrew, J.W.; Ranga, K.; Krishnan, R. A comparison of stereology and segmentation techniques for volumetric measurements of lateral ventricles in magnetic resonance imaging. Neuroimaging 61:53–60; 1995.
12. Jernigan, T.L.; Press, G.A.; Hesselink, J.R. Methods for measuring brain morphologic features on magnetic resonance images: Validation and normal aging. Arch. Neurol. 47:27–32; 1990.
13. Shenton, M.E.; Kikinis, R.; Jolesz, F.A.; Pollak, S.D.; LeMay, M.; Wible, C.G.; Hokama, H.; Martin, J.; Metcalf, D.; Coleman, M.; McCarley, R.W. Abnormalities of the left temporal lobe and thought disorder in schizophrenia. A quantitative magnetic resonance imaging study. New Engl. J. Med. 327:604–612; 1992.
14. Robb, R.A. A software system for interactive and quantitative analysis of biomedical images. In: 3D Imaging in Medicine, NATO ASI Series, F(60). K.H. Möhne, H. Fuchs, and S.M. Pizer (Eds). Springer Verlag NATO ASI Series; 1990:333–361.
15. Mackay, C.E.; Roberts, N.; Mayes, A.R.; Downes, J.J.; Foster, J.K.; Mann, D.; Edwards, R.H.T. An exploratory study of the relationship between face recognition memory and the volumes of medial temporal lobe structures in healthy young males. Behav. Neurol. (in press).
16. Pache, J.C.; Roberts, N.; Vock, P.; Zimmerman, A.; Cruz-Orive, L.M. Vertical LM sectioning and parallel CT scanning designs for stereology: Application to human lung. J. Microsc. 170:3–24; 1993.
17. Thirion, J.-P.; Gourdon, A. The 3D marching lines algorithm. Graphical Models and Image Processing. 58:503–509; 1996.
18. Subsol, G.; Thirion, J.-P.; Ayache, N. Application of an anotomically built 3D morpometric atlas. In: K.H. Hohne and R. Kikinis (Eds). Visualization in Biomedical Computing, number 1131 in Lecture Notes in Computer Science, Hamburg, Germany: Springer Verlag; 1996:373–382.
19. Besl, P.J.; McKay, N.D. A method for registration of 3D shapes. IEEE Transact. Pattern Anal. Machine Intell. 14:239–255; 1992.
20. Zhang, Zh. On local matching of free-form curves. In: D. Hogg and R. Boyle (Eds). Leeds, UK. British Machine Vision Conference, British Machine Vision Association, Springer Verlag; 1992.
21. Pentland, A.; Sclaroff, S. Closed-form solutions for physically based shape modeling and recognition. IEEE Transact. Pattern Anal. Machine Intell. 13:715–729; 1991.
22. Nastar, Ch.; Ayache, N. Fast segmentation, tracking and analysis of deformable objects. In: Proceedings of the Fourth International Conference on Computer Vision (ICCV' 93), Berlin, Germany: IEEE Computer Society Press 1993:275–279.
23. Martin, J.; Pentland, A.; Kikinis, R. Shape analysis of brain structures using physical and experimental modes. In: Computer Vision and Pattern Recognition, Seattle, WA, 1994:752–755.
24. Declerck, J.; Subsol, G.; Thirion, J.-Ph.; Ayache, N. Automatic retrieval of anatomical structures in 3D medical images. In: N. Ayache, (Ed). CVRMed'95, volume 905 of Lecture Notes in Computer Science, Nice, France, Springer Verlag; 1995:153–162.
25. Broca, P. Sur la faculte du language articule. Bull. Mem. Soc. d'Anthropol. Paris 6:377–393; 1865.
26. Hellige, J.B. Hemispheric asymmetry: What's Right and What's Left. Cambridge: Harvard University Press; 1993.
27. Rubens, A.B. Transcortical motor aphasia. In: H. Whitaker and H.A. Whitaker (Eds). Studies in Neurolingu-

istics, vol. 1. New York: Academic Press; 1976:293–303.
28. Baxter, D.M.; Warrington, E.M. Category specific phonological dysgraphia. Neuropsychologia 23:653–666; 1985.
29. Davatzikos, C.; Vaillant, M.; Resnick, S.M.; Prince, J.L.; Letovsky, S.; Bryan, R.N. A computerized approach for morphological analysis of the corpus callosum. J. Comput. Assist. Tomogr. (in press).
30. Bilder, R.M.; Wu, H.; Bogerts, B.; Degreef, G.; Ashtari, M.; Alvir, M.J.; Snyder, P.J.; Lieberman. Ansence of regional hemispheric volume asymmetries in first-episode shizophrenia. Am. J. Psychiatry 10:1437–1447; 1994.
31. Subsol, G.; Thirion, J.-P.; Ayache, N. A general scheme for automatically building 3D morphometric anatomical atlases: Application to a skull atlas. In: Medical Robotics and Computer Assisted Surgery, Baltimore, MD; John Wiley and Sons; 1995:226–233.
32. Székely, G.; Kelemen, A.; Brechbühler, C.; Gerig, G. Segmentation of 3D objects from MRI volume data using constrained elastic deformations of flexible Fourier surface models. In: N. Ayache (Ed). CVRMed'95, volume 905 of Lecture Notes in Computer Science, Nice, France; Springer Verlag; 1995:495–505.
33. Bookstein, F.L. Thin-Plate Splines and the Atlas Problem for Biomedical Images. In: A.C.F. Colchester and D.J. Hawkes (Eds). Information Processing in Medical Imaging, number 511 in Lecture Notes in Computer Science, Wye, UK, Springer Verlag; 1991:326–347.
34. Cootes, T.F.; Taylor, C.J.; Cooper, D.H.; Graham, J. Active shape models—Their training and application. Comput. Vision Image Understand. 61:38–59; 1995.